

UC Irvine

UC Irvine Previously Published Works

Title

Fast ion profiles during neutral beam and lower hybrid heating

Permalink

<https://escholarship.org/uc/item/7b15f0b6>

Journal

Plasma Physics and Controlled Fusion, 28(6)

ISSN

0741-3335

Authors

Heidbrink, WW
Strachan, JD
Bell, RE
[et al.](#)

Publication Date

1986-06-01

DOI

10.1088/0741-3335/28/6/003

Copyright Information

This work is made available under the terms of a Creative Commons Attribution License, available at <https://creativecommons.org/licenses/by/4.0/>

Peer reviewed

FAST ION PROFILES DURING NEUTRAL BEAM AND LOWER HYBRID HEATING

W. W. HEIDBRINK, J. D. STRACHAN, R. E. BELL, A. CAVALLO, R. MOTLEY, G. SCHILLING,
J. STEVENS and J. R. WILSON

Plasma Physics Laboratory, Princeton University, Princeton, New Jersey, U.S.A.

(Received 12 August 1985; and in revised form 21 January 1986)

Abstract—Profiles of the $d(d,p)t$ fusion reaction are measured in the PLT Tokamak using an array of collimated 3 MeV proton detectors. During deuterium neutral beam injection, the emission profile indicates that the beam deposition is as narrow as predicted by a bounce-averaged Fokker-Planck code. The fast ion tail formed by lower hybrid waves (at densities above the critical density for current drive) also peaks strongly near the magnetic axis.

1. INTRODUCTION

THE DEPOSITION of auxiliary power affects the heating and stability of a Tokamak plasma. Measurements of the density of energetic ions created by auxiliary heating can be used to infer the power deposition profile. Previously, the density of energetic ions was studied by measuring the spatial distribution of $d(d,n)^3\text{He}$ fusion reactions during neutral beam (STRACHAN, 1978) and lower hybrid (SCHUSS, 1981) heating. The measurements confirmed that most of the neutrons originated near the center of the Tokamak but accurate profiles were not achieved. An alternative approach to the study of neutral beam deposition is measurement of the emission from impurity lines excited through charge exchange with the beam neutrals. Measurements in PLT indicate that the neutral profile during beam injection peaks strongly near the magnetic axis (SUCKEWER, 1980, 1984; SKINNER, 1984).

In this paper, the profile of fast ions produced by deuterium neutral beam and lower hybrid heating is studied by measuring the $d-d$ fusion emission profile with an array of collimated 3 MeV proton detectors (HEIDBRINK, 1985). During $D^0 \rightarrow D^-$ neutral beam injection, the fusion emission is principally due to beam-target reactions and the reaction rate profile yields information on the location of the injected beam ions during the initial phases of their slowing down. The results are consistent with Fokker-Planck calculations of the beam deposition.

Fusion reaction rate profiles were also measured during lower hybrid heating of a PLT deuterium plasma at a density where the fusion reactivity was enhanced by the formation of an ion tail. In this case, the fusion reactions are due to the energetic ion tail created by the lower hybrid waves. The results indicate that the wave damping on ions is centrally located and that the fast-ion tail probably only dissipates a small fraction of the applied lower hybrid power.

2. PROTON DIAGNOSTIC

This paper presents experimental results obtained by measuring 3 MeV protons produced in $d(d,p)t$ fusion reactions with an array of collimated silicon surface barrier detectors. This 3 MeV proton diagnostic has been described elsewhere (HEIDBRINK, 1985) so only a brief description is presented here. The detectors are mounted near

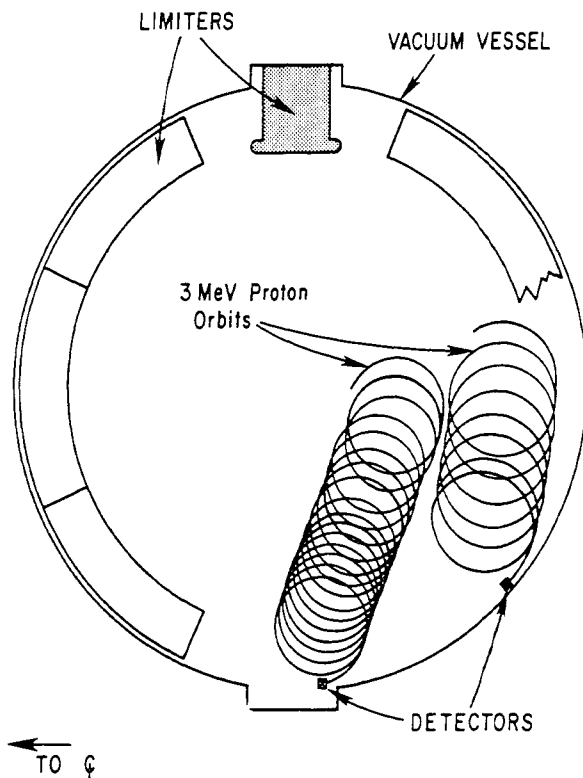


FIG. 1.—Poloidal projection of two proton orbits measured by the PLT array of 3 MeV proton detectors. The protons are measured by collimated ($\text{FWHM} \approx 5^\circ$) surface barrier detectors mounted near the bottom of the vacuum vessel. The limiters are vertically symmetric and centered about $R = 132$ cm.

the bottom of the PLT vacuum vessel. Together with the magnetic field, the orientation and collimation of the detectors determine the orbits of protons measured by each detector. The array of proton detectors can be thought of as a set of curved vertical “chords” looking up through the plasma (Fig. 1). The number of protons measured by a detector is related to the fusion emissivity through an inversion algorithm that includes geometrical factors for the area and collimation of the detector, and that relies on numerical calculations of proton orbits (HEIDBRINK, 1985). The accuracy of the inversion is enhanced by the strong central peaking of the fusion emission.

A major uncertainty in relating the proton data to the fusion emissivity is uncertainty in the position of the center of the emission. The nominal position of the magnetic axis is expected to be about 135 cm for a well-positioned PLT plasma with a Shafranov shift of about 3 cm. Measurements of the sawtooth inversion radii made by tilting the angle of the grating of an ECE polychromator (FISCHER, 1983) in ohmic discharges similar to the ones studied here found that the inversion radii were centered at 136 ± 3 cm. The neoclassical orbit shift Δ of tangential beam ions is $\Delta \approx 1.3$ cm. Measurements of the neutron emission with a poloidal array of indium foils during $D^0 \rightarrow D^+$ neutral beam injection found that the emission was centered at $R_0 = 140 \pm 1$ cm (ZANKL, 1981). In their analysis, ZANKL *et al.* did not include the effect on the poloidal

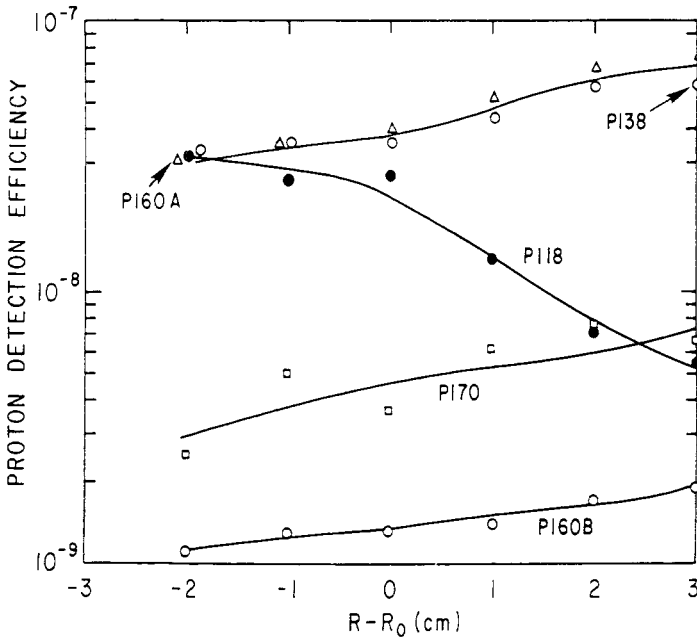


FIG. 2.—Proton detection efficiency [proton counts divided by $d(d,n)$ emission] versus horizontal plasma position during $D^0 \rightarrow D^-$ neutral beam injection in PLT. Each point is the average of the proton detection efficiency over the 200 ms of beam injection; the statistical error for $\epsilon = 10^{-8}$ is typically $\pm 5\%$. The curves are fits to the data.

neutron flux of the anisotropy of the $d(d,n)^3\text{He}$ fusion reaction (JARMIE, 1985). Including anisotropy, we find that Zankl's data imply that the emission was centered at $R_0 = 137 \pm 2$ cm. In our analysis (Section 3), we have used $R_0 = 138$ cm, which is consistent with all of the proton data and with the other measurements of the plasma center. If the emission profile was actually centered closer to the nominal center of the plasma, then the main effect on the data plotted in Figs. 3 and 4 is to shift the points 2–3 cm farther out in minor radius with little change in their relative position or magnitude.

3. RESULTS

The data presented here are from clean (Spitzer conductivity $Z_{eff} \simeq 1.5$), high field ($B_\phi \simeq 31$ kG), deuterium PLT discharges. The discharges were programmed so that the plasma current ($I_p = 450$ kA) and electron density ($\bar{n}_e = 1.6 \times 10^{13}$ cm^{-3} during neutral beam injection and $\bar{n}_e = 1.3 \times 10^{13}$ cm^{-3} during lower hybrid) were constant beginning 200 ms before the auxiliary heating and throughout the 200 ms (150 ms) neutral beam (lower hybrid) pulse. At the relatively low power levels employed ($P_B = 140$ kW; $P_{LH} = 240$ kW), the auxiliary power had little ($< 5\%$) effect on the electron energy content of the plasma; the most obvious effect of the heating on the plasma was a factor of one hundred (factor of four) increase in the d–d neutron emission during the neutral beam (lower hybrid) pulse. The neutral beam power and voltage ($W_b = 23.7$ keV) were set to prevent pulse pileup in the 3 MeV proton detection electronics.

3.1. Deuterium neutral beam injection

A measurement of the emission profile during neutral beam heating was obtained by comparing the fluence of the various proton detectors as a function of position. A second, essentially independent, measurement of the emission profile was obtained by moving the plasma small amounts radially via changes in the equilibrium vertical field (Fig. 2). The plasma position was moved shot-to-shot in increments of 1 ± 0.1 cm in a series of discharges in which the other plasma parameters were maintained nearly constant. The PLT plasma was limited by mushroom-shaped carbon rail limiters above and below the plasma at $r = 40$ cm and by carbon "bumper" limiters at $r = 42$ cm in the major radial direction (Fig. 1). Changes in radial position of the plasma of $\lesssim 2$ cm are not expected to affect the core plasma significantly. Since the neutron emission and electron temperature and density did not vary with plasma position, the slope of the fluence as a function of position is related to the gradient of the emission profile.

The emission profile during co-injection of deuterium neutral beams deduced from the data of Fig. 2 is plotted in Fig. 3(a). The profile is deduced from the raw data by guessing an emission profile that is consistent with the measured neutron emission, calculating the expected proton signals and radial gradients with an orbit code (HEIDBRINK, 1985), and iterating until agreement with the data is obtained. Included in Fig. 3(a) is the gradient of the emission deduced from the vertical field scan. The $D^0 \rightarrow D^+$ emission profile is considerably broader than the ohmic emission profile (figure 17 of HEIDBRINK, 1985) but is still strongly peaked near the magnetic axis.

During deuterium neutral beam injection into a deuterium plasma ($D^0 \rightarrow D^+$), the fusion emission is dominated by beam-target fusion reactions (STRACHAN, 1981). Roughly, the emissivity S is determined by the injection energy W_b , the deposition of full-energy beam ions \dot{n}_b , the density of target ions n_d , and the time it takes injected beam ions to slow down due to Coulomb drag (τ_s) (STRACHAN, 1981):

$$S \propto \dot{n}_b n_d \sigma v \tau_s. \quad (1)$$

For beam-target reactions, the reactivity $\overline{\sigma v}$ can be approximated by $\overline{\sigma v} \simeq \sigma v (W_b + c T_i)$, where $c = 4.8$ for $W_b = 23.7$ keV. Since the beam energy is much larger than the ion temperature ($W_b/T_i \gtrsim 20$), the fusion reactivity varies less than 50% over the central half of the discharge. The slowing-down time varies inversely with electron density ($\tau_s \propto n_e^{-1}$), so the emissivity does not depend on the magnitude of the plasma density but only on the deuterium concentration ($S \propto n_d/n_e$). For these PLT discharges with $Z_{eff} \simeq 1-1.5$, it is reasonable to assume that the deuterium depletion (n_d/n_e) is independent of position. Thus, equation (1) implies that, for these conditions, the emission profile depends most strongly on the deposition profile of full-energy beam ions with a relatively weak dependence on the density and temperature profiles of the bulk plasma. The strongly peaked emission profile [Fig. 3(a)] implies, therefore, that the beam deposition \dot{n}_b peaks strongly near the magnetic axis [Fig. 3(b)].

Also plotted in Fig. 3(a) is the fusion emission profile predicted by a code that employs a fit to the measured electron profiles in a bounce-averaged Fokker-Planck calculation (STRACHAN, 1981; GOLDSTON, 1975). The hatched region in the figure indicates variations in the prediction associated with uncertainties in the neutral density, ion temperature, and electron density profiles. The output of the code has

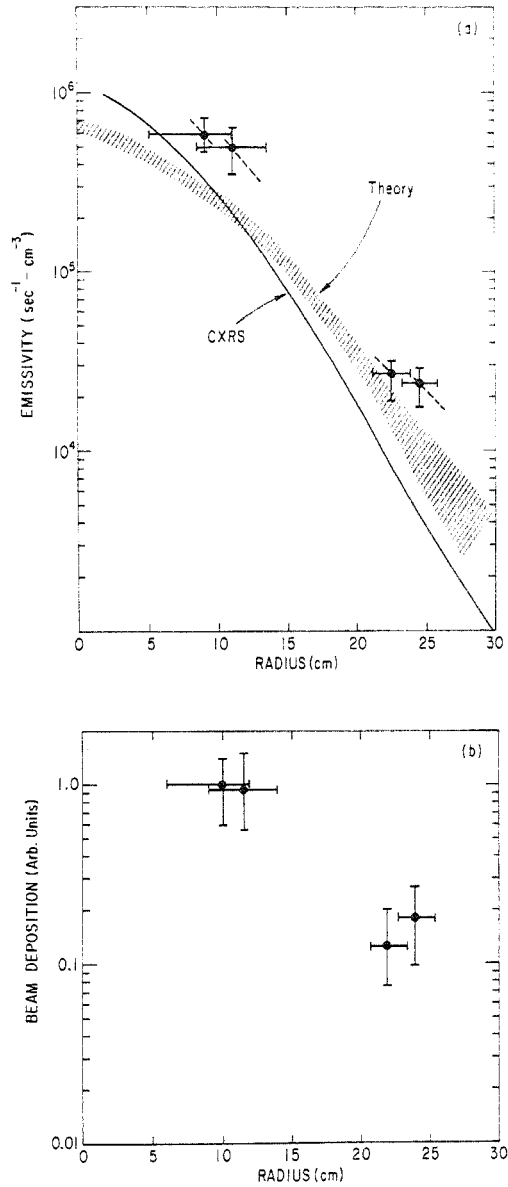


FIG. 3.—(a) 3 MeV proton emissivity versus minor radius during $D^0 \rightarrow D^+$ neutral beam injection on PLT. The proton data are averaged over the 200 ms of beam injection. The dotted lines are the gradient of the emissivity deduced from Fig. 2. The hatched region is the profile predicted by a bounce-averaged Fokker-Planck calculation (STRACHAN, 1981) of the fusion emission. Fits to the Thomson scattering profiles of electron temperature and density were used in the theoretical calculation. The beam neutral deposition was assumed to be the deposition measured in a test stand (GRISHAM, 1977). Also shown (solid line) is the lower limit of the fusion profile predicted by the Fokker-Planck code when the more narrow neutral deposition implied by spectroscopic measurements on PLT (SUCKEWER, 1984) is used in the calculation. The theoretical curves are normalized to equal the neutron emission.
 (b) Density of reacting beam ions n_b deduced using equation 1.

been normalized to agree with the neutron emission, which is measured with an absolute accuracy of $\pm 40\%$. The total emission implied by the proton measurements is about a factor of two greater than measured by the neutrons but the two measurements are consistent within experimental uncertainties. Comparison of the shape of the theoretical curve with the proton measurements indicates that the beam deposition is as narrow as theoretically predicted. Measurements on PLT of the radiation from impurities that charge exchange with beam neutrals found that the vertical radius of half intensity of the beam neutrals was 6 ± 2 cm (SUCKEWER, 1984), which is narrower than expected from measurements of the divergence of the neutral beams on a test stand (GRISHAM, 1977). Calculations indicate that the fusion emission profile is sensitive to the divergence of the beam [Fig. 3(a)]. Within the experimental uncertainties, the proton measurements are consistent with either neutral deposition profile.

3.2. Lower hybrid

The d(d,p)t emission profile was measured during application of 240 kW of lower hybrid power (800 MHz) to a plasma with $\bar{n}_e = 1.3 \times 10^{13} \text{ cm}^{-3}$. The phase difference between adjacent waveguides for this experiment was 60° , which excited a spectrum of waves with high parallel phase velocity ($n_{\parallel} \simeq 1-5$). The effect of the lower hybrid waves was to enhance the d(d,n)³He reaction rate at densities between $\bar{n}_e = 1.0-1.5 \times 10^{13} \text{ cm}^{-3}$ due to the formation of a fast ion tail (SCHUSS, 1981; CHRIEN, 1983). At $\bar{n}_e = 1.3 \times 10^{13} \text{ cm}^{-3}$, the reaction rate was enhanced by a factor of four. The d(d,p)t emission profile was observed to remain very strongly peaked on axis [Fig. 4(a)] during application of the lower hybrid power.

The 3 MeV proton spectra during the lower hybrid (HEIDBRINK, 1984) were similar to the one measured previously on PLT (CHRIEN, 1983). During the ohmic heating phase the width of the spectra was limited by the instrumental resolution, but during the lower hybrid the spectral width was determined by the energies of the reacting deuterons. Defining the mean energy of the reacting deuterons as the deuteron energy implied by the width of the spectrum at half-maximum (HEIDBRINK, 1984),

$$\langle E_d \rangle = \frac{8(\text{HWHM})^2}{3 \cdot 4.04 \text{ MeV}}, \quad (2)$$

where HWHM is the half-width of the spectrum after correction for broadening from noise, the spectral measurements indicate that the mean energy of the reactants was probably not larger near the magnetic axis than away from it [Fig. 4(b)].

In general, the emissivity could be larger in the center of the plasma either because the fast ions are more energetic there or because the number density of fast ions is higher in the center of the device. Since the Doppler broadening is not greater in the center of the plasma than farther out [Fig. 4(b)], the peaking of the emission profile suggests that the number density of tail ions is an order of magnitude greater in the center of the plasma than about 15 cm farther out.

Assuming that the acceleration of the ion tail by the lower hybrid is balanced by Coulomb drag, it is possible to estimate the profile of wave damping on fast ions.

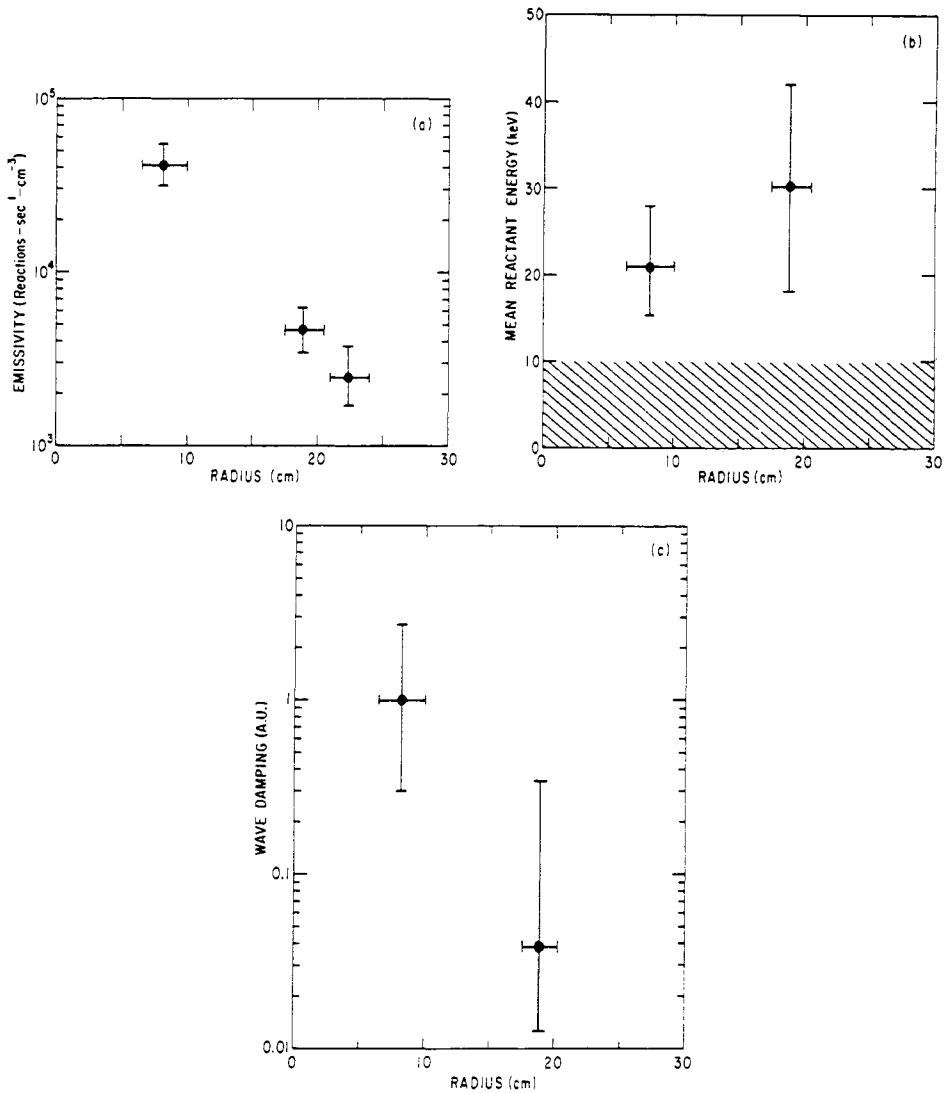


FIG. 4.—(a) 3 MeV proton emissivity versus minor radius during lower hybrid heating. The data are the average over the steady-state portion (140 ms) of thirteen reproducible discharges. (b) Average energy of the reacting deuterons deduced from the 3 MeV proton spectra during lower hybrid heating as a function of position. The hatched region indicates the instrumental resolution. (c) Wave damping on ions versus minor radius assuming that acceleration by the waves is balanced by Coulomb drag (SPITZER, 1962). The error is dominated by uncertainty in the reactivity σv .

The damping is given by the number of tail ions n_t times their energy loss rate $\hat{c}E_t \cdot \hat{c}t$.

$$n_t \frac{\hat{c}E_t}{\hat{c}t} \simeq \left(\frac{S}{\sigma v n_d} \right) \frac{\hat{c}E_t}{\hat{c}t} \propto \frac{S}{\sigma v n_d \tau_s}. \quad (3)$$

Taking the deuterium depletion (n_d/n_e) as constant and using the measurements of

Fig. 4(a) for S , the proton spectral measurements [Fig. 4(b)] to infer $\overline{\sigma v}$, and Thomson scattering measurements for T_e , gives the ion damping profile of Fig. 4(c). Within experimental uncertainties, most of the energy absorbed by the ion tail is deposited near the magnetic axis.

The peaked proton emission profile measured here [Fig. 4(a)] is consistent with the neutron profile measured during lower hybrid on Alcator-A (SCHUSS, 1981). CHRIEN *et al.* (1983) found that in PLT the fast ion tail accounted for only about 10% of the total ion energy content. They assumed that the tail ions lose energy through Coulomb damping in the plasma center and estimated that the fast ions probably only dissipate about 1% of the applied lower hybrid power. In Alcator-A, it was suggested that the inefficient bulk heating during lower hybrid might be due to losses of the fast ions in ripple wells (SCHUSS, 1983). Because of the smaller ripple and larger plasma current in PLT, however, central ~ 30 keV deuterons are expected to be confined, so our observation that the deuterium tail is in the center of the plasma supports the conclusion that these ions only dissipate a small fraction of the applied lower hybrid power under these conditions.

4. CONCLUSION

The beam deposition on PLT was found to be as narrow as theoretically predicted and the ion tail formed during lower hybrid also peaked strongly near the magnetic axis.

Acknowledgements—We thank J. HOSEA and the PLT group for their support, G. ESTEPP for technical assistance, and R. GOLDSTON and J. LOVBERG for helpful discussions. This work was supported by U.S. Department of Energy Contract No. DE-AC02-76-CHO-3073.

REFERENCES

- CHRIEN R. E., KAITA R. and STRACHAN J. D. (1983) *Nucl. Fusion* **23**, 1399.
 FISCHER J. *et al.* (1983) *Rev. scient. Instrum.* **54**, 1085.
 GOLDSTON R. J. (1975) *Nucl. Fusion* **15**, 651.
 GRISHAM L. R., TSAI C. C., WHEALTON J. H. and STIRLING W. L. (1977) *Rev. scient. Instrum.* **48**, 1037.
 HEIDBRINK W. W. (1984) Tokamak Diagnostics using Fusion Products, Ph.D. Thesis, Princeton Univ. 158.
 HEIDBRINK W. W. and STRACHAN J. D. (1985) *Rev. scient. Instrum.* **56**, 501.
 JARMIE N. and BROWN R. E. (1985) *Nucl. Instrum. Meth.* **B10**, 405.
 SCHUSS J. J. *et al.* (1981) *Nucl. Fusion* **21**, 427.
 SCHUSS J. J., ANTONSEN Jr., T. M. and PORKOLAB M. (1983) *Nucl. Fusion* **23**, 201.
 SKINNER C. H. *et al.* (1984) *Phys. Rev. Lett.* **53**, 458.
 SPITZER Jr., L. (1962) *Physics of Fully Ionized Gases*, Interscience, New York.
 STRACHAN J. D. *et al.* (1978) *Phys. Lett.* **66A**, 295.
 STRACHAN J. D. *et al.* (1981) *Nucl. Fusion* **21**, 67.
 SUCKEWER S. *et al.* (1980) *Phys. Rev. A* **22**, 725.
 SUCKEWER S. *et al.* (1984) *App. Phys. Lett.* **45**, 236.
 ZANKL G., STRACHAN J. D., LEWIS R., PETTUS W. and SCHMOTZER J. (1981) *Nucl. Instrum. Meth.* **185**, 321.
 These authors quote an emission profile centered at $R_0 = 142$ cm but they take the geometrical center of the vacuum vessel as 134 cm rather than the design value (132 cm) used here.